Yiting Xie, Shuang Liu, Albert Miller, Jeffrey A. Miller, Steven Markowitz, Ali Akhund, and Anthony P. Reeves "Coronary artery calcification identification and labeling in low-dose chest CT images", Proc. SPIE 10134, Medical Imaging 2017: Computer-Aided Diagnosis, 101340L (3 March 2017)

https://doi.org/10.1117/12.2254125

Coronary artery calcification identification and labeling in low-dose chest CT images

Yiting Xie[a], Shuang Liu[a], Albert Miller[b], Jeffrey A. Miller[c], Steven Markowitz[b], Ali Akhund[b], and Anthony P. Reeves[a]

[a]School of Electrical and Computer Engineering, Cornell University, Ithaca, NY, USA
[b]Barry Commoner Center for Health and the Environment, Queens College, City University of New York, Queens, NY, USA
[c]School of Medicine, Rutgers University, Newark, NJ, USA

ABSTRACT

A fully automated computer algorithm has been developed to evaluate coronary artery calcification (CAC) from low-dose CT scans. CAC is identified and evaluated in three main coronary artery groups: Left Main and Left Anterior Descending Artery (LM + LAD) CAC, Left Circumflex Artery (LCX) CAC, and Right Coronary Artery (RCA) CAC. The artery labeling is achieved by segmenting all CAC candidates in the heart region and applying geometric constraints on the candidates using locally pre-identified anatomy regions. This algorithm was evaluated on 1,359 low-dose ungated CT scans, in which each artery CAC content was categorically visually scored by a radiologist into none, mild, moderate and extensive. The Spearman correlation coefficient R was used to assess the agreement between three automated CAC scores (Agatston-weighted, volume, and mass) and categorical visual scores. For Agatston-weighted automated scores, R was 0.87 for total CAC, 0.82 for LM + LAD CAC, 0.66 for LCX CAC and 0.72 for RCA CAC; results using volume and mass scores were similar. CAC detection sensitivities were: 0.87 for total, 0.82 for LM + LAD, 0.65 for LCX and 0.74 for RCA. To assess the impact of image noise, the dataset was further partitioned into three subsets based on heart region noise level (low<=80HU, medium=(80HU, 110HU], high>110HU). The low and medium noise subsets had higher sensitivities and correlations than the high noise subset. These results indicate that location specific heart risk assessment is possible from low-dose chest CT images.

Keywords: coronary artery calcification identification and labeling, low-dose chest CT, automated computer algorithm

1. INTRODUCTION

Coronary artery calcification (CAC) is an indicator of coronary heart disease, which is the most common type of heart disease and is responsible for the death of over 370,000 people annually in the US[1]. Evaluating CAC content in a lung cancer screening cohort that have annual low-dose CT (LDCT) scans may be beneficial since the participants are also at high risk of heart disease; however, identifying and labeling the CAC regions in these scans is more challenging than in traditional cardiac CT scans due to cardiac motion and high image noise and for which only initial visual scoring techniques have been established[2-3]. In this paper, we present a fully automated algorithm that segments the CAC from low-dose chest CT scans and labels CAC by artery, which is then compared to radiologist categorical visual scores.

Tota-Maharaj et al.[4] have indicated that increased number of vessels with CAC improved the diagnostic power of the traditional CAC Agatston score. They manually labeled and scored CAC content by 4 main arteries: Left Main (LM), Left Anterior Descending (LAD), Left Circumflex (LCX) and Right Coronary Artery (RCA). They also demonstrated that LM and LAD CAC had independent prognostic significance in predicting mortality. Automated labeling of CAC by artery has been developed for ECG-triggered cardiac CT scan[5-6]. Ding et al.[5] used atlas registration and active contours to segment heart region and surrounding vessels. Then CACs were labeled using a knowledge-based region separation algorithm. Wolterink et al.[6] used a feature classification method to label individual CAC. Both algorithms combined LM and LAD CAC into one label due to the difficulty to visually distinguish CAC at the border of LM and LAD[6] and comparison in these studies was made with semi-automated CAD Agatson scores.

Medical Imaging 2017: Computer-Aided Diagnosis, edited by Samuel G. Armato III, Nicholas A. Petrick,
Proc. of SPIE Vol. 10134, 101340L · © 2017 SPIE · CCC code: 1605-7422/17/$18 · doi: 10.1117/12.2254125

In the context of LDCT, there have been several studies for obtaining the overall CAC content[7-9]. This work extends our previous algorithm[9] to evaluate CAC content in 3 main artery groups in LDCT: LM + LAD, LCX and RCA. CAC candidates were automatically segmented and partitioned into these 3 groups and 3 types of automated CAC scores (Agatston-weighted, volume, and mass) were computed for all CACs and by arteries. The algorithm was evaluated on a screening cohort of 1,359 ungated LDCT scans. In each scan, CAC content was visually scored per artery by a radiologist using the recommended categorical scoring method[3]. The visual scores were compared to the automated CAC scores and the Spearman correlation coefficient was computed. Detection sensitivities and specificities were also computed. To study the effect of image noise on CAC detectability, the cohort was further partitioned into 3 subsets based on heart region noise level and the same measurements were performed.

2. METHODS

The algorithm consists of the following steps: 1) image filtering and thresholding to obtain all CAC candidates in the heart region; 2) excluding non-CAC candidates using geometric constraints; 3) labeling remaining CAC candidate based on geometric constraints with respect to local labeled anatomy.

(1) Image filtering and thresholding for CAC candidate extraction

Low-pass image filtering has been optimized to remove the impact of noise without filtering out the evidence for CAC. Heart region noise is automatically measured as the pixel standard deviation in the segmented heart region. Currently a 3x3 mean filter is used for images with moderate to high noise level (heart region noise<=150HU) and a 5x5 mean filter is used for those with very high noise level (heart region noise above 150HU) based on empirical evidence. Threshholding is set at the standard threshold of 130 HU in the superior region of the heart and this is increased to 180 HU in the inferior region due to increased noise.

(2) Exclusion of non-CAC candidates

Common types of non coronary artery calcification and high-intensity artifacts are excluded based on geometric locations. They include: aorta calcium on the segmented aorta surface, calcium or artifacts in the transition region between lung and heart, aortic valve calcium close to ascending aorta root region, and mitral valve calcium in the posterior heart region. Figure 1 shows examples of excluded non-CAC candidates.

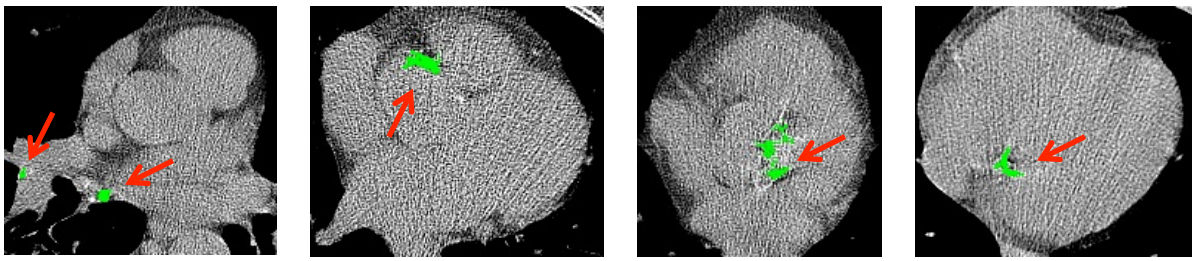

(a) (b) (c) (d)

Fig. 1. Examples of excluded non-CAC candidates (green regions indicated by red arrows): (a) calcium in the transition region between lung and heart; (b) aortic calcium; (c) aortic valve calcium; (d) mitral valve calcium.

(3) Labeling of CAC candidates by artery

CAC labeling relies on the geometric constraints from pre-segmented anatomy regions such as the aorta, heart and pulmonary trunk[9-10]. The general labeling model is shown in Figure 2 (a) and (b). Labeling starts from the most obvious and robustly identified CAC regions (RCA and LM + LAD) and use them to provide constraints to the more subtle CAC regions. Details are described below.

1: Labeling of RCA CAC.

The RCA is well defined by the inferior ascending aorta (AA_i) and the inferior heart (Hrt_i). It is also constrained by a smaller distance to the right lung compared to the left lung ($R_{ldist}>3*R_{rdist}$) as shown in Figure 2 (c)).

2: Labeling of LM + LAD CAC adjacent to aorta.
For the left CACs, the algorithm first searches for CAC adjacent to the ascending aorta (AA) in its posterior left region (AA_{ang}=4 in Figure 2(f)). This belongs to LM + LAD and is usually the most easily identified CAC on the left side and can provide a robust constraint to other left CACs. CACs in this region are constrained by a small distance to AA (AA_{dist}) as well as the superior heart (Hrt_s) and the inferior AA ($AA_i + d_1$). They are also constrained by a smaller distance to the left lung (L_{ldist}<L_{rdist}). Figure 2 (d)-(f) show the model in this region.

3: Labeling of other LM + LAD and LCX CAC.
If CAC is detected in step 2, a simple anterior/posterior partition model is used to separate the remaining CACs into LAD and LCX (see Figure 3 (a)). However, if no CAC is detected in step 2, CAC adjacent to pulmonary trunk (see Figure 3 (b)) or CAC anterior to AA center (see Figure 3 (c)) is used to establish the anterior/posterior partition between LAD and LCX.

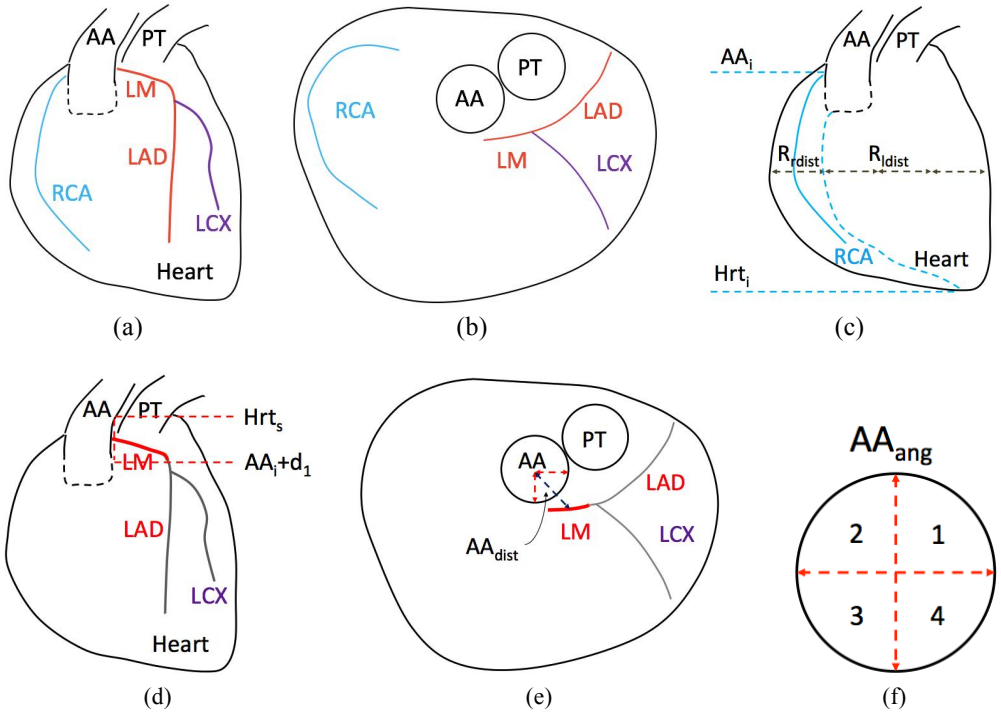

Fig. 2. Illustration of geometric model for CAC labeling. (a) and (b) show the locations of coronary arteries in heart with ascending aorta (AA) and pulmonary artery trunk (PT). (c) shows the RCA CAC labeling model. (d) and (e) show the labeling model for CAC adjacent to AA while (f) illustrates the AA_{ang} computation.

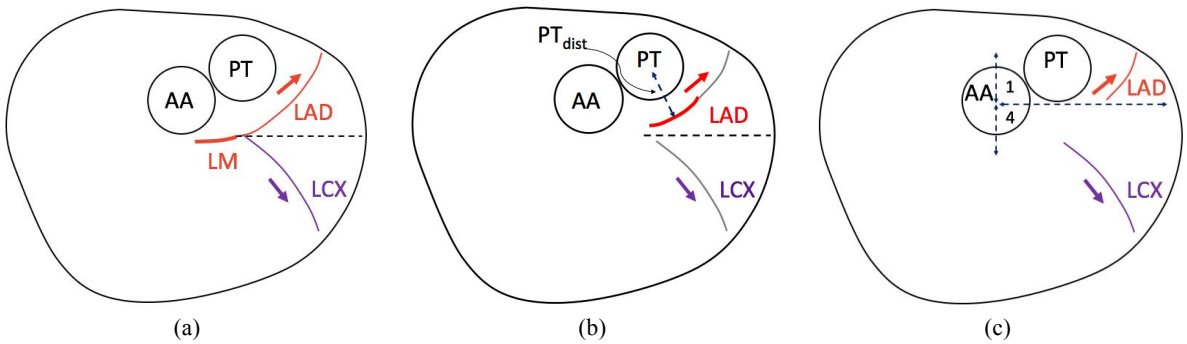

Fig. 3. Labeling of other left CACs in different scenarios: (a) shows the partition model when LM + LAD CAC adjacent to AA exists; (b) shows the partition model using CAC adjacent to PT; (c) shows the partition model using CAC anterior to AA center.

3. DATA

The dataset consists of 1,437 CT scans from different subjects. Scans with severe metal implant artifacts (18 scans) or unacceptable heart region segmentation (60 scans) were excluded. The remaining 1,359 scans were used for analysis and evaluation. All scans were taken using SIEMENS Emotion16 scanners and reconstructed with a B70s kernel at a slice thickness of 2mm. The scans were acquired with either 110 or 130 kVp and a current ranging from 50 to 183 mA (1,137 cases with a current ≤ 84 mA).

Each scan was assigned a categorical visual CAC score for each of the four arteries (LM, LAD, LCX, RCA) by a radiologist using the criteria established by Shemesh et al.[3]. The score categories are: none=0, mild=1, moderate=2, extensive=3. In our assessment, the visual scores of LM and LAD were added together for LM + LAD CAC assessment. The visual scores of all four arteries were added together for total CAC assessment. Figure 4 shows example cases with 4 different visual scores for each artery.

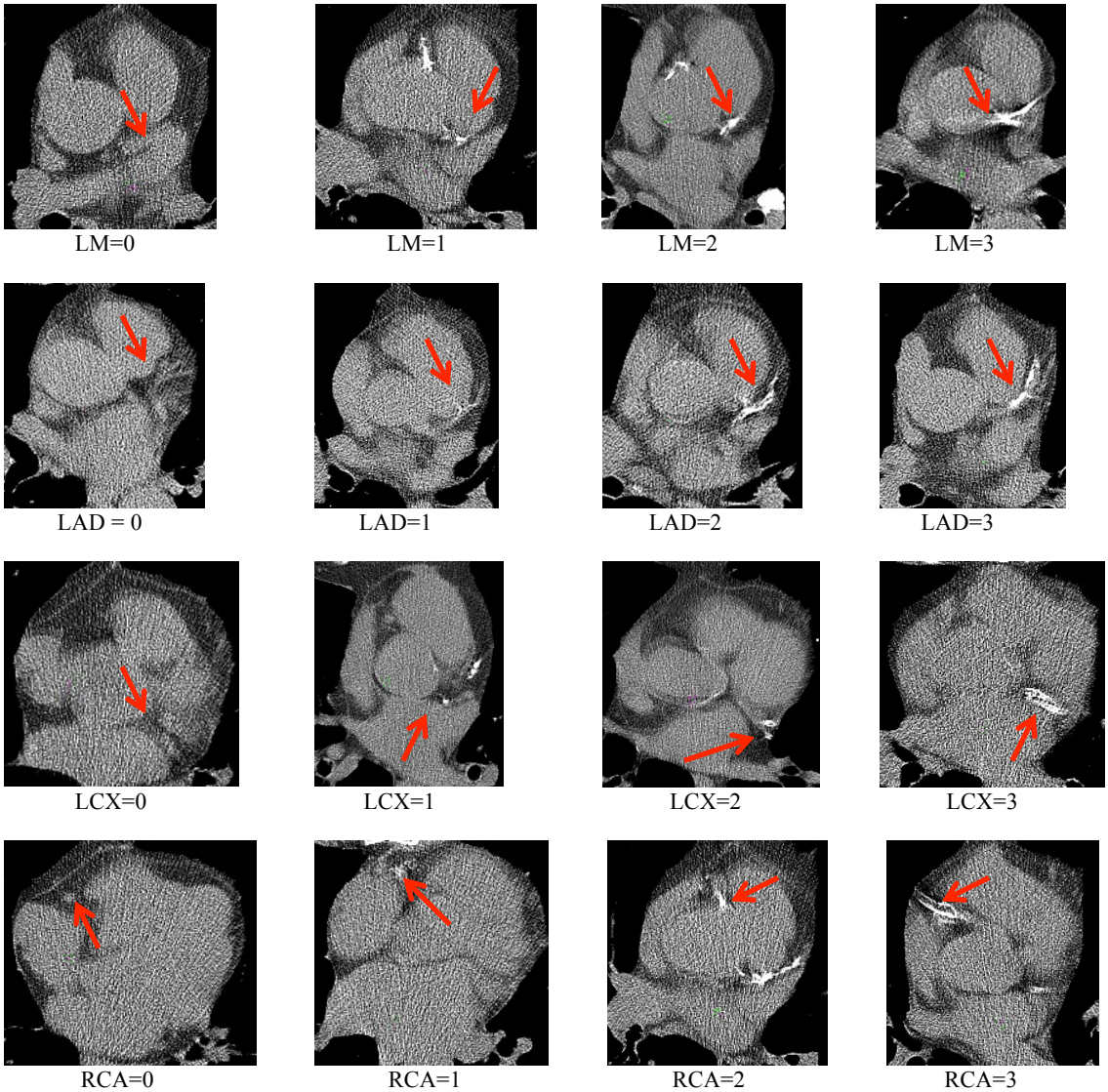

Fig. 4. Example cases with different levels of visual scores for each artery: none=0, mild=1, moderate=2, extensive=3. Red arrows indicate the artery (CAC) location in each image.

4. EXPERIMENTS

Two experiments were performed to evaluate the algorithm. The first experiment evaluated the agreement between the categorical visual scores of the radiologist and three automated CAC scores (an Agatston-weighted score, a volume score, and a mass score) by computing their Spearman correlation coefficient R (total and by artery). The second experiment determined the labeling performance of the system by evaluating the sensitivity, specificity, positive predictive value and negative predictive value of CAC labeling by artery. For each artery, a true positive (TP) occurs when both the automated and visual scores are non-zero; a false positive (FP) occurs when only the automated score is non-zero; a false negative (FN) occurs when only the visual score is non-zero and a true negative (TN) occurs when they are both zeroes. Sensitivity is defined as TP/(TP+FN), specificity is defined as TN/(FP+TN), positive predictive value (PPV) is defined as TP/(TP+FP), and negative predictive value (NPV) is defined as TN/(TN+FN).

Higher noise level usually leads to the decrease of sensitivity and overall performance of the algorithm. In order to evaluate the impact of noise on the outcome, the cohort (1,359 scans) were further divided into three subsets based on the noise level: low noise group 398 cases <= 80HU, medium noise group 499 cases = 80-110HU, and high noise group 462 cases > 110HU. Noise level was automatically measured in the segmented heart region by taking the standard deviation. The threshold of 80HU and 110HU were chosen so that each subset would contain similar number of cases. The two experiments were repeated for all subsets and the same set of results were reported.

4. RESULTS

Results on the whole dataset with 1,359 scans are shown in Table 1 and Table 2. Table 1 shows correlations with visual scores and Table 2 shows sensitivities, specificities, positive predictive values and negative values for all CACs and by artery. Statistics of the Agatston-weighted scores are summarized in Table 3.

Table 1. Spearman correlation coefficient R between visual scores and automated Agatston-weighted, volume and mass scores for all CACs and by artery.

Spearman R	#Cases	All CACs	LM+LAD CAC	LCX CAC	RCA CAC
Visual v.s. Agatston-weighted	1,359	0.87	0.82	0.66	0.72
Visual v.s. Volume	1,359	0.88	0.82	0.66	0.73
Visual v.s. Mass	1,359	0.87	0.82	0.66	0.72

Table 2. Labeling sensitivity, specificity, positive predictive value (PPV) and negative predictive value (NPV) for all CACs and by artery.

Metric	#Cases	All CACs	LM + LAD CAC	LCX CAC	RCA CAC
Sensitivity	1,359	0.87	0.82	0.65	0.74
Specificity	1,359	0.84	0.89	0.92	0.88
PPV	1,359	0.94	0.95	0.86	0.83
NPV	1,359	0.67	0.64	0.77	0.81

Table 3. Statistics of Agatston-weighted scores for all CACs and by artery.

Agatston-weighted	#Cases	All CACs	LM + LAD CAC	LCX CAC	RCA CAC
Mean	1,359	391.9	213.5	78.76	99.7
Median	1,359	71.0	35.0	0	0
Range	1,359	[0, 6328.0]	[0, 3657.0]	[0, 4105.0]	[0, 4836.0]
Standard-deviation	1,359	762.5	428.1	321.8	321.9

Results on the three subsets with different noise levels are in Table 4 and 5 and Figure 6. Among the 1,359 scans, the mean noise level in the heart region is 102HU as shown in Figure 5 (median = 96HU, range = [39HU, 313HU], standard deviation = 36HU).

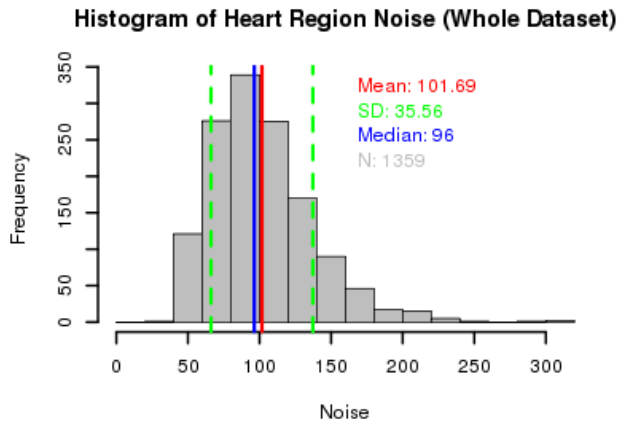

Fig. 5. Histogram of heart region noise distribution on the whole dataset (1,359 cases).

Table 4. Spearman correlation coefficient R between visual scores and automated Agatston-weighted, volume and mass scores for all CACs and by artery for the three noise level subsets. Low noise = 1 (398 cases), medium noise = 2 (499 cases), high noise = 3 (462 cases).

Spearman R	All CACs			LM+LAD CAC			LCX CAC			RCA CAC		
	1	2	3	1	2	3	1	2	3	1	2	3
Visual v.s. Agatston-weighted	0.87	0.90	0.85	0.83	0.85	0.80	0.68	0.65	0.67	0.74	0.74	0.69
Visual v.s. Volume	0.88	0.90	0.86	0.83	0.85	0.80	0.68	0.65	0.68	0.75	0.74	0.69
Visual v.s. Mass	0.87	0.89	0.85	0.83	0.85	0.80	0.68	0.65	0.67	0.74	0.73	0.69

Table 5. Labeling sensitivity, specificity, positive predictive value (PPV) and negative predictive value (NPV) for all CACs and by artery for the three noise level subsets. Low noise = 1 (398 cases), medium noise = 2 (499 cases), high noise = 3 (462 cases).

Metric	All CACs			LM+LAD CAC			LCX CAC			RCA CAC		
	1	2	3	1	2	3	1	2	3	1	2	3
Sensitivity	0.90	0.89	0.82	0.87	0.85	0.74	0.66	0.66	0.63	0.74	0.78	0.70
Specificity	0.84	0.86	0.83	0.84	0.91	0.91	0.94	0.90	0.92	0.90	0.87	0.88
PPV	0.94	0.95	0.94	0.93	0.96	0.96	0.88	0.85	0.87	0.84	0.82	0.82
NPV	0.74	0.72	0.57	0.74	0.70	0.53	0.80	0.77	0.75	0.82	0.84	0.78

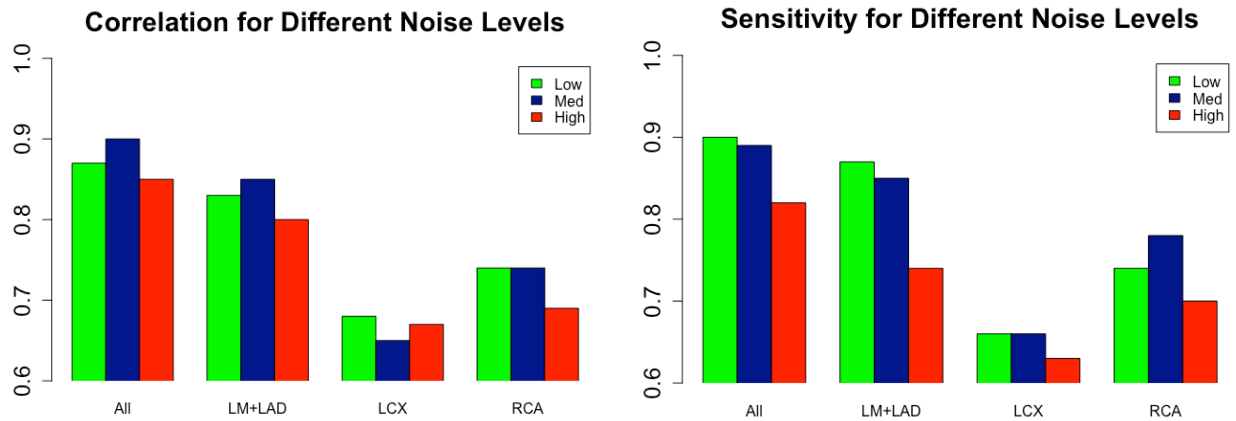

Fig. 6 Bar plots to illustrate the difference of correlation and sensitivity between the three noise groups.

Pearson Chi-squared test was used to compare the sensitivity differences. The following sensitivities were significantly different from each other (p-value < 0.05): all CACs low v.s. high (p = 0.008); all CACs medium v.s. high (p = 0.009); LM + LAD CACs low v.s. high (p < 0.001); LM + LAD CACs medium v.s. high (p < 0.001).

5. DISCUSSION

Segmenting and labeling of CAC in LDCT is challenging because the actual coronary arteries are not detectable unless they contain (usually a small amount of) calcium. The very high noise level present in these scans also makes it hard to extract any representative image features from these small CAC regions. Thus, the algorithm labels CACs based on their geometric relationship with respect to other pre-identified organs. The most robustly identified CACs are first labeled, based on which the locations of the remaining CACs are identified. The algorithm shows agreement with visual scores (R=0.82, 0.66 and 0.72 by artery). Sensitivities were 0.82, 0.65, and 0.74 by artery. Figure 7 shows two examples of correctly identified CACs.

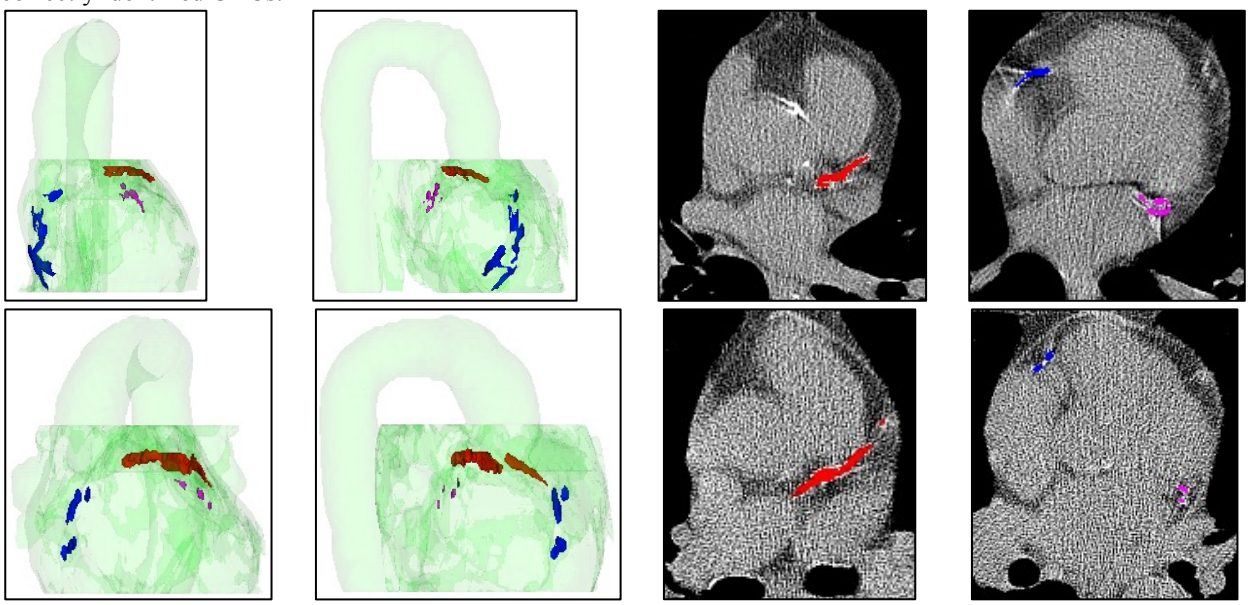

(a) (b) (c) (d)

Fig. 7. Examples of correctly labeled CAC in two cases (upper and lower rows). (a) and (b) shows a coronal and a sagittal view with heart and aorta region in light green, LM + LAD CAC in red, LCX CAC in magenta, and RCA CAC in blue. (c) and (d) shows axial slices with labeled CACs using the same color scheme.

CAC segmentation errors occur in a small number of cases where geometric location alone cannot distinguish CAC from other calcium in proximity. In these cases, the automated algorithm over-segments by including non-coronary artery calcium close to coronary arteries (see Figure 8 (b)). CAC labeling errors sometimes occur between LM + LAD and LCX CACs. This is most likely to happen where LM branches into LAD and LCX (see Figure 8 (c)).

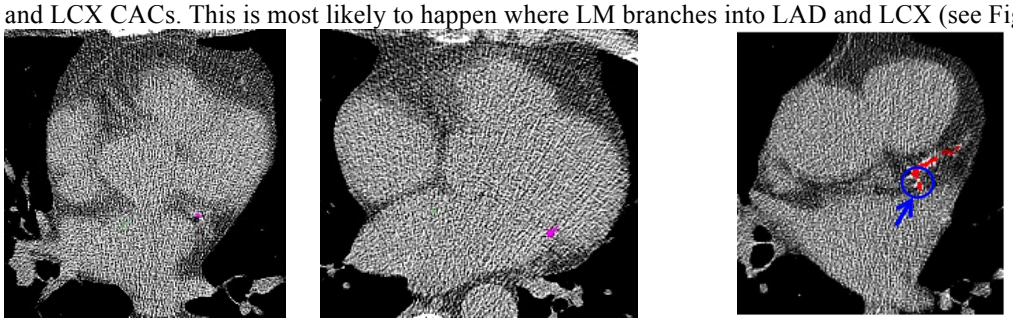

(a) (b) (c)

Fig. 8. Examples of CAC segmentation and labeling errors. (a) and (b) show labeled LCX CAC in magenta. (a) is correctly labeled while (b) is a false positive. (c) shows LCX CAC (inside blue circle) mistaken as LM + LAD CAC.

CAC detection sensitivities of the low and medium subsets were significantly different from that of the high noise subset for all CACs and LM + LAD CACs (see Table 4 and 5). There was no significant difference between the low and medium noise subsets. The overall sensitivity decreased from 0.89 to 0.82 and the correlation coefficient decreased from 0.87 to 0.85. Among the three artery groups, LCX CACs had the lowest correlation and detection sensitivity. There are a number of reasons: LCX contained the smallest amount of calcium (see Table 3) and therefore was most easily impacted by image filtering and image noise; a large amount of LCX CACs located near the branching point of LM (see Figure 8 (c)), causing confusion and error.

6. CONCLUSION

In conclusion, a fully automated algorithm has been developed to segment and label CAC from LDCT scans. Evaluated on 1,359 LDCT images, the fully automated algorithm detected most CAC regions and the automated Agatston-weighted, volume and mass scores showed similar good correlation with the categorical visual scores assigned by the radiologist (Agatston-weighted score R=0.87 for total, and 0.82 for LM+LAD, 0.66 for LCX and 0.72 for RCA). The labeling algorithm has the potential to aid cardiac health assessment by providing the additional information of CAC scores in individual arteries in the context of low-dose ungated CT images of the chest, thus serving the large at-risk population that is undergoing lung cancer screening.

ACKNOWLEDGMENTS

This study was supported in part by the Flight Attendant Medical Research Institute (FAMRI).

REFERENCES

[1] http://www.cdc.gov/heartdisease/facts.htm (accessed June 1st, 2016).
[2] Shemesh, J., Henschke, C. I., Farooqi, A., Yip, R., Yankelevitz, D. F., Shaham, D., and Miettinen, O. S. “Frequency of coronary artery calcification on low-dose computed tomography screening for lung cacner.” Clinical Imaging. 30(3): 181-185 (2006).
[3] Shemesh, J. Henschke, C.I., Shaham, D., Yip, R., Farooqi, A.O., Cham, M.D., McCauley, D.I., Chen, M., Smith, J.P., Libby, D.M., Pasmantier, M.W., and Yankelevitz, D.F. “Ordinal scoring of coronary artery calcifications on low-dose CT scans of the chest is predictive of death from cardiovascular disease.” Radiology. 257(2): 541-548 (2010).
[4] Tota-Maharaj, R., Joshi, P.H., Budoff, M.J., Whelton, S., Zeb, I., Rumberger, J., Al-Mallah, M., Blumenthal, R.S., Nasir, K., and Blaha, M. J. “Usefulness of Regional Distribution of Coronary Artery Calcium to Improve the Prediction of All-Cause Mortality.” AJC. 115(9): 1229-1234 (2015).
[5] Ding, X., Slomka, P. J., Diaz-Zamudio, M., Germano, G., Berman, D. S., Terzopoulos, D., and Dey D. “Automated Coronary Artery Calcium Scoring from Non-contrast CT Using a Patient-specific Algorithm,” SPIE Medical Imaging. 9413, 94132U (2015).
[6] Wolterink, J. M., Leiner, T., Takx, R. A.P., Viergever, M. A., and Isgum, I. “Automatic Coronary Calcium Scoring in Non-Contrast-Enhanced ECG-Triggered Cardiac CT With Ambiguity Detection,” IEEE Trans Med Imaging. 34(9): 1867-1878 (2015).
[7] Isgum, I., Prokop, M., Niemeijer, M., Viergever, M.A., and van Ginneken, B. “Automatic coronary calcium scoring in low-dose chest computed tomography.” IEEE TMI. 31(12): 2322-2334 (2012).
[8] Takx, R.A.P., de Jong, P.A., Leiner, T., Oudkerk, M., de Koning, H.J., Mol, C.P., Viergever, M.A., and Isgum, I. “Automated Coronary Artery Calcification Scoring in Non-Gated Chest CT: Agreement and Reliability.” PLOS ONE. 9(3): e91239 (2014).
[9] Xie, Y., Cham, M. D., Henschke, C., Yankelevitz, D., and Reeves, A. P. “Automated coronary artery calcification detection on low-dose chest CT images.” SPIE Medical Imaging. 9035, 90350F (2014).
[10] Xie, Y., Liang, M., Yankelevitz, D. F., Henschke, C. I., and Reeves, A. P. “Automated measurement of pulmonary artery in low-dose non-contrast chest CT images.” SPIE Medical Imaging. 9414, 94141G (2015).